Tabula Rasa: Oxygen precipitate dissolution though rapid high temperature processing in silicon

Erin E. Looney[1], Hannu S. Laine[1,2], Mallory A. Jensen[1], Amanda Youssef[1], Vincenzo LaSalvia[3], Paul Stradins[3], Tonio Buonassisi[1]

[1]Massachusetts Institute of Technology, Cambridge, MA 02139, USA, email: elooney@mit.edu
[2]Department of Electronics and Nanoengineering, Aalto University, Tietotie 3, 02150 Espoo, Finland
[3]National Renewable Energy Laboratory, Golden, CO 80401, USA

Abstract — **Over one fourth of all monocrystalline silicon ingots suffer from a 20% performance degradation due to oxygen precipitates. Tabula Rasa (TR) is a mitigation technique that dissolves these precipitates, making them harmless. This work explores the dependence of oxygen dissolution on annealing time and temperature for the TR process to aid in solar cell process optimization. The dissolution time for oxygen precipitates was found to be more than 10 minutes for total dissolution, longer than normal TR process times in the electronics industry. The activation energy, extracted from the precipitate dissolution curves, is found to be 2.6 ± 0.5 eV. This value when compared to the migration enthalpy of oxygen in silicon can be used to reveal the energy limiting proces in TR.**

Index terms **– oxygen related defects, monocrystalline silicon, *tabula rasa*, thin wafering, precipitate dissolution**

I. Introduction

The capital expenditure (capex) required to manufacture photovoltaic modules is a central barrier to the rapid adoption of solar technologies needed to meet climate targets [1]. One strategy to reduce the capex is to increase manufacturing yield. The majority of industrial mono-crystalline silicon is made with the Czochralski (Cz-Si) method which comprises 35-40% of the current solar material used today [2]. Between 25-30% of typical Cz-Si ingots are afflicted with a specific defect that accounts for a 20% relative drop or around 4% absolute reduction in conversion efficiency for this material [3]. The portion of the ingot inflicted with these defects , called "ring" or "swirl" defects are sorted out as lower quality material. The "swirl" defects are in reality several types of micro defects that are caused by the interplay of silicon interstitials, vacancies, oxygen precipitates, and other intrinsic point defects during the solidification of the silicon ingot [4].

Oxygen is the most abundant impurity in Cz-Si, usually present at 10-20 ppma in solar cell material. Oxygen in as-grown material takes several forms ranging from interstitial oxygen with low recombination activity to strained oxide precipitates with high recombination activity [5]-[6]. During cell fabrication, high temperature steps such as phosphorus diffusion gettering, thermal oxidation, and firing introduce the wafer to temperatures that allow the oxygen to change between these different states, and therefore reduce the minority carrier lifetime in the material [7].

Process optimization tools have been developed to mitigate detrimental effects of most metal impurities, for example iron defect control during phosphorus diffusion gettering and firing have been optimized using kinetic models [8]. However, currently no such process or modeling tools exist for mitigating the effects of oxygen in the solar industry, partly due to the insufficient quantification of the dissolution kinetics of oxygen in silicon for solar applications.

We work to solve this problem through the study of *tabula rasa* (TR), meaning "blank slate," which is a rapid high temperature process between 1090 – 1150°C maintained for 1-2 minutes aimed at mitigating these defects [9]. In the integrated circuit (IC) industry this process is used to install a certain vacancy profile in the wafer, while erasing the thermal history, leaving silicon wafers "blank slates" as all oxygen is left in interstitial form with no precipitates or nuclei [10]. The solar industry does not incorporate such an anneal before cell processing, leaving as-grown defects that formed during the crystallization process to evolve throughout the high temperature process steps of cell fabrication. By using an optimized TR process on an industrial cell fabrication line, it is hypothesized that these oxygen-related swirl defects can be dissolved, reclaiming the 20% relative drop in efficiency in the affected portion of each Cz-Si ingot and thus improving manufacturing yield [11]. In this work, the dissolution kinetics of the TR process have been quantified so that accurate modeling and optimization can be realized to accomplish this yield gain.

II. Methods

A. Materials

We use 745 µm thick, *p*-type, 200 mm diameter, double side polished, electronic-grade Cz-Si wafers with a resistivity of 10-12 Ω-cm resistivity. The wafers contain negligible extrinsic impurities other than oxygen content of 13.75 ppma. These wafers are laser cut into 3.5x3.5 cm^2 rectangles for oxygen precipitate growth. After chemical cleaning for metal and organic contaminants, each sample undergoes a series of high temperature steps in an N_2 atmosphere, quartz tube furnace to nucleate and grow large oxygen precipitates in a homogeneously distributed pattern [12]. The time-temperature profile can be seen in Fig. 1, and includes a nucleation step at 550 °C for 6 hours, precipitate growth steps at 800°C for 4 hours, 925°C for 4 hours, and 1000°C for 16 hours, and lastly ambient cooling to 700°C before being pulled out of the furnace. The samples are then cleaved into smaller 1x1 cm^2 pieces, chemically etched with CP4 and HF-dipped to remove any surface damage or oxide left from the high temperature processing.

978-1-5090-5605-7/17/$31.00 ©2017 IEEE

B. Experiment

A series of TR processes are performed on the samples at five temperatures between 1100°C and 1290°C. For each temperature, TR experiments were performed at six different times between 1 and 30 minutes. We expect the highest temperature, longest time TR process (1290°C for 30 minutes) to completely dissolve the grown-in oxygen precipitates, and for the shortest time, lowest temperature process (1100°C for 1 minutes) to dissolve the precipitates the least. The TR process is done in a horizontal mullite tube furnace (N_2 ambient) with temperatures measured from external thermocouples and a disappearing filament optical pyrometer. The push and pull rate both into and out of the furnace was 10 seconds, and the samples sat at the end of the furnace for 10 seconds before being put on a large silicon heat sink and cooled in ambient air. The samples were then HF dipped to remove any oxide formed on the surface.

C. Characterization

The oxygen distribution in the wafer was characterized using Fourier Transform Infrared Spectroscopy (FTIR) to quantify interstitial oxygen $[O_i]$ concentration and chemical etching to reveal oxygen precipitates [13]. FTIR was used to determine $[O_i]$ concentration before precipitate growth, after precipitate growth, and after the TR step shown in Fig. 1. These measurements were calibrated using ASTM standard 121-83. After the growth process depicted in Fig. 1, the interstitial oxygen content was measured at 5.35 ppma, down from the total oxygen before the anneal at 13.75 ppma, or 6.88×10^{17} atoms/cm^3, indicating that 61% of oxygen atoms precipitated during growth. Through chemical defect etching done for 45 seconds (HF:CH_3COOH:HNO_3 with a volume ratio of 36:15:2), the precipitate density is determined to be 1.6×10^9 ppt/cm^3 by counting etch pits in a representative volume. Assuming that the oxygen precipitates are all of similar size and spherical, using the radius of an oxygen atom, $r = 6.5 \times 10^{-9}$ cm, the oxygen precipitates are calculated to have a diameter between 70-90 nm or 2-3 x 10^8 oxygen atoms per precipitate. Finally, after each TR step, FTIR is performed again to determine how many of these precipitates have dissolved back into interstitial oxygen. Using these methods, the macro scale character of the oxygen including total, interstitial, and precipitated density and size is determined for each point in the process.

III. Results

Fig. 2 plots $[O_i]$ concentration as a function of annealing time for each TR temperature. As expected, interstitial oxygen concentration increases steadily at each TR temperature, due to dissolution of oxygen precipitates. To quantify the dependence of the dissolution rate on TR temperature, dissolution curves for the oxygen precipitates are plotted in **Fig. 2**. The dissolution time constant, τ_{diss}, was determined for each temperature by fitting the interstitial oxygen data with the equation:

$$[Oi]\,(t) \propto C_s\left[1 - \exp\left(-\frac{t}{\tau_{diss}}\right)\right] \qquad (1)$$

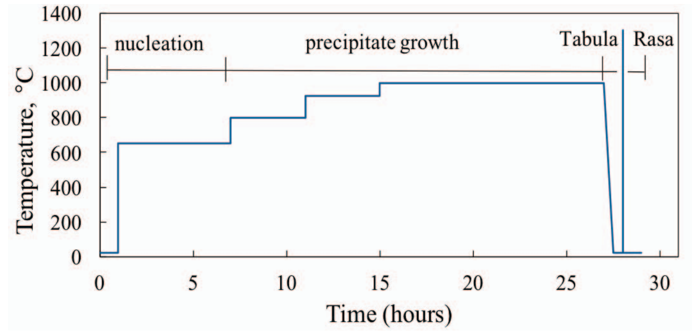

Fig. 1 Time-temperature profile for wafer preparation and experiment.

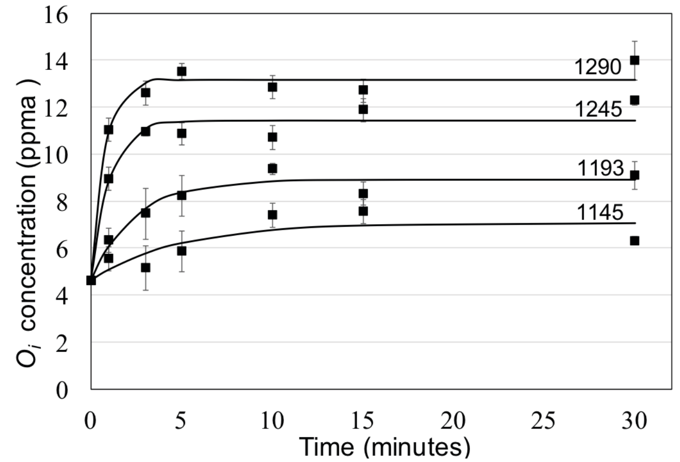

Fig. 2 Dissolution curves are plotted as interstitial oxygen content for four temperatures and six times. The dissolution time constant ranged from around 1 to 6 minutes between the temperatures, and none of the temperatures managed to completely dissolve the precipitates to $[O_i]$ = 13.75 ppma which is the total oxygen content of the samples.

where, C_s is the observed saturation concentration of interstitial oxygen at each TR temperature.

The four curves plotted in Fig. 2 represent the four TR process temperatures and demonstrate the dissolution of oxygen precipitates at a steep initial rate with a saturation at a certain concentration. The solid solubility limit of interstitial oxygen in silicon is not reached during the longest 30-minute TR run for any of these temperatures except for the 1145°C curve using the intrinsic solubility described by $9 * 10^{22} \exp\left(\frac{-1.52\ eV}{kT}\right) cm^{-3}$ [14]. The 1100°C curve is not plotted as it shows no change in concentration, because the solid solubility at this temperature (4.74 ppma) is close to the starting concentration of $[O_i]$ for these samples. At 1193°C and 1245°C, the $[O_i]$ concentration reaches a steady dissolution rate below their solid solubility limits.

Our explanation for this behavior is that the process has become kinetically limited and the size of the oxygen precipitates in these samples is too large to dissolve quickly with a TR step at these temperatures. The traditional TR process is around 1050—1200°C for 1—5 minutes and would not be sufficient. It is observed that for TR to be an effective process,

the appropriate time and temperature for complete dissolution of oxygen precipitates must be used. This profile must take into consideration the oxygen content and morphologies within the as-grown wafer.

The activation energy for dissolution, E_a, was found using the fitted dissolution time constants, τ_{diss}, and fitting these to an Arrhenius-type temperature-dependent equation.

$$\frac{1}{\tau_{diss}} \propto \exp\left(\frac{E_a}{k_b T}\right) \quad (2)$$

The activation energy indicates the limiting physical process in dissolution. If the activation energy is larger than the diffusion coefficient for interstitial oxygen in silicon, then there is an additional physical process limiting the dissolution process. This could be, for example, the dissolution reaction in which one oxygen atom breaks away from a precipitate (reaction-limited dissolution). If the activation energy is found to be close to the migration enthalpy, then the diffusion of an oxygen atom away from a precipitate is interpreted to be the limiting step, and no significant extra energy is needed to dissolve precipitates greater than the kinetic limitations of diffusion [15]. If the activation energy is smaller than the migration enthalpy, then the dissolution of oxygen precipitates is enhanced, decreasing the energy needed for an oxygen atom to break from a precipitate and diffuse away. The activation energy was found to be 2.6 ± 0.5 eV which is within the range of the migration enthalpy for $[O_i]$ in silicon which is 2.53 ± 0.3 eV [14]. This information can be used to reveal the limiting energy for the TR process, and dissolution of oxygen precipitates can be modeled based on known kinetic and solubility material properties without any extra energy barrier.

IV. Industry Impact

The TR process is a promising solution to the issue of yield loss for Cz solar cells due to oxygen-related defects. To justify such a high temperature process step, predictive process modeling capabilities are key to implementation. This work enables this modeling as oxygen dissolution during TR is shown to be kinetically limited. To realize this model for industry, efficient methods for characterization of the as-grown oxygen distributions are in development. Work on more reliable and nondestructive techniques for oxygen precipitate characterization is ongoing [16]. With as-grown oxygen distributions characterized and the physics behind dissolution now quantified, time-temperature profiles can be optimized to put oxygen into the least recombination active form.

V. Conclusions

The activation energy of oxygen dissolution was determined to be in the same range as the coefficient of diffusion, ~2.6 eV. This information can be used to infer the limiting physical process in the dissolution. The oxygen dissolution saturates before the solid solubility limit. From that saturation point, the precipitates slowly dissolve after an initially quick dissolution rate because the oxygen precipitates are above the critical radius for that temperature. This explains why none of the TR processes fully dissolved the precipitates with diameters averaging 70 nm. For other material, including industrial PV materials, shorter and lesser temperature processes are possible if the material has smaller oxygen precipitates. Knowledge of the size and density of the oxygen precipitates within the wafer is needed to determine which TR process is appropriate.

References

[1] D. Berney Needleman, *et al., Ener. & Environ. Sci.*, **9**, 2016.
[2] "ITRPV: Results 2015," VDMA PV Equipment, 2016.
[3] J. Haunschild, *et al.,* Phys. Status Solidi RRL **5**, 2011.
[4] V. V. Voronkov, Jour. of Crys. Growth, **59**, pp. 625–643, 1982.
[5] J. Michel, *et al., Semicond. & Semimet.*, **42**, 1994.
[6] R. Falster, *et al., Mat. Sci. Forum,* **573-574**, pp. 45–60, 2008.
[7] J. D. Murphy, *et al., Solid State Phenomen.*, **178–179**, 2011.
[8] J. Hofstetter, et al. Prog. in PV: Res. and App. 2011; **19**
[9] V. LaSalvia *et al.,* 2016 IEEE 43rd PVSC, 2016.
[10] G. Kissinger *et al.*, *Jour. of Electrchem. Soc.,* **154**, 2007.
[11] B. Sopori *et al.*, *IEEE Jour. of PV,* **7**, 2017.
[12] R. J. Falster, Montgomery Research Group Europe, **12**, 2002.
[13] B. Sopori, *et al., Jour. of Electrchem. Soc.,* **131**, 1984.
[14] J. C. Mikkelsen, *MRS Proceedings*, **59**, 1985.
[15] F. Shimura, *Appl. Phys. Letters*, **39**, 1981.
[16] A. Youssef, *et al.,* accepted talk, *Silicon PV,* 2017.